





Adsorption of Zirconium Ions by X-Type Zeolite

Hanna Vasylyeva ^{1,*}, Ivan Mironyuk ², Mykola Strilchuk ³, Volodymyr Tryshyn ^{3,4}, Olexander Gaidar ^{3,4}, Oleksander Vasyliiev ⁵

¹ Department of Theoretical physics, Uzhgorod National University, 14 Universytetska Str., 88000, Uzhgorod, Ukraine; h.v.vasylyeva@hotmail.com (H.V.);

² Department of Chemistry, Vasyl Stefanyk Precarpathian National University, 57 Shevchenko Str., 76018 Ivano Frankivsk, Ukraine; myrif555@gmail.com (I.M.);

³ Institute for Nuclear Research of NAS Ukraine, Laboratory of Nuclear Forensics, Nauky Avenue 47, Kyiv, Ukraine; myst@kinr.kiev.ua (M.S.);

⁴ Institute for Nuclear Research of NAS Ukraine, CEPAE, Nauky Avenue 47, Kyiv, Ukraine; vtryshyn@kinr.kiev.ua (V.T.);

⁵ Institute of Electron Physics of NAS Ukraine, 21 Universytetska Str., 88017, Uzhgorod, Ukraine; nucleargoga@gmail.com (O.V.);

* Correspondence: h.v.vasylyeva@hotmail.com (H.V.);

Scopus Author ID 65061599572

Received: 8.01.2021; Revised: 2.02.2021; Accepted: 5.02.2021; Published: 13.02.2021

Abstract: Dependence of zirconium adsorption value on agitation time, solution acidity, equilibrium concentrations of zirconium cations, and zeolite NaX particle size was investigated. The two most common adsorption theories Langmuir and Freundlich, were used to analyzing equilibrium adsorption data. Nonlinear approximation shows that the Freundlich adsorption theory provides higher R^2 and lower χ^2 for zirconium adsorption by NaX than the Langmuir adsorption theory. Experimental maximum adsorption values of NaX toward zirconium and strontium cations are $75 \text{ mg}\cdot\text{g}^{-1}$ and $156 \text{ mg}\cdot\text{g}^{-1}$ respectively. The desorption studies of zirconium ions from the surface of NaX by 1% oxalic acid and 10% HNO_3 were performed. Degradation of the adsorbent in nitric acid was studied in a batch mode. The recovered suspended particles filter cake was investigated by X-ray fluorescence analysis. Alumina oxide (Al_2O_3) fraction decreases, and MgO is completely washed out from the adsorbent matrix in concentrated HNO_3 .

Keywords: zirconium; zeolite; adsorption; dissolution; strontium.

© 2021 by the authors. This article is an open-access article distributed under the terms and conditions of the Creative Commons Attribution (CC BY) license (<https://creativecommons.org/licenses/by/4.0/>).

1. Introduction

Radioactive materials and radionuclides are widely used in science, education, medicine, atomic energy, etc. Radioactive contamination can be a result not only of NPP facility but also of nuclear weapons testing. Over the last 50 years, several inorganic adsorption materials are used to purify water solutions from radionuclides, for example, from ^{90}Sr or ^{60}Co [1-9]. Zeolites are crystalline hydrated aluminosilicates. Synthetic and natural aluminosilicates occupy an essential place among other silicon-based adsorbents such as titanium silicate [10], nano-sized stannic silicomolybdate [11], or fumed silica [12, 13], which are offered for adsorption of heavy metals cations and radionuclides from aqueous solutions. The unique structure of zeolites makes them attractive for various practical applications, including gas and vapor separations, membrane reactors, chemically selective adsorption, and slow-release fertilizers in agriculture [14]. ^{90}Sr adsorption onto modified zeolites over the past 10 years is described in publication [4]. The structure of zeolites can be modified with heavy metal cations, such as Cu^{2+} , to enhance the adsorption and catalytic properties [15]. Many natural, synthetic,

and modified zeolites were proposed for the adsorption of heavy metal cations such as Pb^{2+} , Cd^{2+} , Cu^{2+} , Mn^{2+} , Ni^{2+} , Pb^{2+} , Zn^{2+} , and NH_4^+ [1-5, 16-22]. The high adsorption capacity of zeolites, relative to strontium cations, and high radiation resistance, have led to the use of zeolite NaX as a carrier for ^{90}Sr [1].

On the other hand, among the many scientific papers on zeolites, few works are devoted to the adsorption of zirconium ions by zeolites. Zirconium is a well-known radiation resistance metal dopant because of its small neutron capture cross-section. It is widely used in alloys from which the core of nuclear reactor housings are made. Zirconium has several isotopes. Some of them are being used for medical purposes; for example, ^{89}Zr is used as a positron emitter in PET diagnostic. Isotopes of $^{92-95}\text{Zr}$ can be produced as fission radionuclides during uranium nuclear fission. Therefore, isotopes of $^{92-95}\text{Zr}$, along with ^{90}Sr , can be found in radioactive waste. Ion exchange resins DOWEX 50WX4 is usually proposed for the adsorption of zirconium ions, as well as compounds based on silicon or biowaste rice bran. Extraction, chelation, or adsorption of zirconium ions by hydroxamate resin is offered to isolate zirconium for medical purposes [23-26].

Our research reviews zirconium adsorption by zeolite NaX compares obtained results versus strontium adsorption in similar conditions and studies zirconium desorption and NaX degradation in acid medium.

2. Materials and Methods

In the present work, commercial synthetic NaX zeolite was used. Zeolite NaX relates to the faujasite topology (FAU). The main source material for NaX is kaolin [27-30]. NaX lattices have a network of pores with a diameter of nearly 7,4 -8 Å. In NaX, 'X' means that Si/Al ratio in zeolite equals 1-1,4. According to [31], the zeolite Si/Al ratio plays a universal role in the acid medium's zeolite's stability. All chemical compounds, including ZrOCl_2 , NaX, NH_4OH , HNO_3 , $\text{SrCl}_2 \cdot 6\text{H}_2\text{O}$, and oxalic acid ($\text{H}_2\text{C}_2\text{O}_4 \times 2\text{H}_2\text{O}$), were of reagent grade and used without further purification. Distilled and deionized water was obtained using a three-stage water purification system.

2.1. XRF analysis.

The chemical composition of zeolite NaX and Si/Al ratio were confirmed by fluorescent X-ray analysis using S2Ranger ©2010 Bruker AXS (Karlsruhe, Germany). The XRF analysis was provided with voltage 50kV; tube current 1000 μA ; pressure 1000 mBar; filter 250 mm Cu. The spectrometer records a "number of count" N versus 2θ , the position of the detector. This 2θ position can be converted in the wavelength λ with the Bragg's law, and photon E's energy (the energy of photons and the wavelength of the radiation are linked by the Planck's constant). The content of corresponding elements, was determined by KA1 lines with energy of 1,041 keV (Na); 1,25keV (Mg); 1,74keV (Si); 1,48 keV (Al); 3,69keV (Ca); 4,511 keV (Ti); 14,166 keV (Sr); 15,6 keV (Zr).

2.2. Determination of the point of zero charges.

The point of zero charges of the NaX surface was determined using the drift method. 100 mg of NaX was added to 15 ml 0,1 M NaCl solution and the ionic strength was kept constant in all experiments. The initial pH value was adjusted from 2,0 to 11,0 by adding 0,1M HCl or KOH solutions. The solutions were kept for 24 hours. The final pH value was measured

using pH meter with a glass electrode. The point of zero charges was considered at a straight-line $pH_{final} = pH_{initial}$ cross with the experimental curve pH_{final} versus $pH_{initial}$. Point of zero charge of NaX surface has $pH=11,5$.

2.3. Adsorption and desorption studies.

Adsorption investigations were performed in a batch mode with the liquid: solid (L: S) phase ratio equal to 50 ($m_{ads} = 0,1$ g; $V_{sol} = 5$ ml). To investigate desorption efficiency, the adsorption study was performed at standard conditions. After adsorption, the samples of NaX were washed with deionized distilled water. Then it was dried at room temperature. For the desorption study, a given mass (approximately 0,1g) of NaX was washed in 10 ml of various desorbing agents. This study's desorbing agents included 10% HNO_3 , concentrated HNO_3 , and 1% oxalic acid.

The initial and residual concentration of stable isotopes of zirconium was determined using direct complexometric titration in a strong acid medium with Xylenol Orange as an indicator. XRF analysis of zeolite samples before and after adsorption was performed, as well. The amounts of adsorbed zirconium ions were calculated using equation (1) according to [8, 32-35]:

$$q_e = \frac{[(C_o - C_e)V]}{m} \quad (1)$$

Where q_e – is the amount of zirconium uptake, mg/g; C_o and C_e – are initial and residual concentrations of zirconium, mg; V - is solution volume, L; and m - is mass adsorbent, g.

Experimental data of adsorption kinetics were analyzed using models based on pseudo-first and pseudo-second-order equations, Elovich chemisorption kinetic model, and the Weber-Morris intra-particle diffusion kinetic model. Corresponding equations (2-5) are given in Table 1.

Table 1. Linear analytical equations of kinetic models (2)-(5).

Kinetic model	Linear equation
Elovih	$q_t = \frac{1}{b} \ln(ab) + \frac{1}{b} \ln(t)$ (2)
Diffusion	$q_t = D_{ipd} \times t^{1/2} + k_0$ (3)
Pseudo - first order	$\log(q_0 - q_t) = \log q_0 - k_1 t / 2.303$ (4)
Pseudo-second order	$\frac{t}{q_t} = 1/k_2 q_0^2 + t/q_0$ (5)

q_0 and q_t (mg/g) - adsorption capacity at equilibrium and time t , respectively; k_1 (min^{-1}), k_2 ($\text{g} \cdot \text{mg}^{-1} \cdot \text{min}^{-1}$) rate coefficients of pseudo-first order equation and pseudo-second order equation. D_{ipd} ($\text{mg/g} \cdot \text{min}^{0,5}$) – coefficient of intra-particle diffusion; β (mg/g)- desorption constant, α (mg/g min) – rate coefficients of Elovich equation.

The equilibrium adsorption studies were performed under agitation times not less than 120 minutes. Nonlinear approximation of the experimental results was carried out by the Langmuir and Freundlich theories using the "Solver add-in" application to Microsoft Excel office program, according to [34, 35]. The equations for both theories are given below:

$$q_e = \frac{A_\infty K C_e}{1 + K C_e} \quad (6)$$

$$q_e = K_f \times C_e^n \quad (7)$$

where, A_∞ – maximal adsorption value, which corresponds of fill in the whole adsorption centers, mg/g; K_L – Langmuir equation's constant, L/mg; C_e – adsorbate equilibrium concentration, mg/L; q_e – the amount of adsorbate uptake at equilibrium, mg/g; K_f – Freundlich constant, $\frac{\text{mg/g}}{(\frac{\text{mg}}{\text{L}})^n}$; n - Freundlich intensity parameter.

Arithmetic mean and error of arithmetic mean were calculated using program [36], with the confidence level of 99%. Values of R^2 and χ^2 were calculated by equations (8) and (9).

$$R^2 = 1 - \frac{\sum(q_{e,exp} - q_{e,calc})^2}{\sum(q_{e,exp} - q_{e,mean})^2} \quad (8)$$

$$\chi^2 = \sum \frac{(q_{e,exp} - q_{e,calc})^2}{q_{e,calc}} \quad (9)$$

The effect of solution acidity on adsorption processes was investigated using a certain amount of HNO₃ or NH₄OH. The acidity of solutions was controlled by the pH-meter "Belarus" 2003".

3. Results and Discussion

3.1. Dependence of zirconium ion adsorption on interaction time and the equilibrium concentration of zirconium ions in a neutral medium.

It has been shown that adsorption values increase with the increased duration of interactions. Equilibrium establishes after 100 minutes of contact between the zeolites surface and zirconium ions (Figure 1). The experimental data of zirconium adsorption by NaX fits well in the Lagergren pseudo-second-order kinetic model ($R^2=0,999$) and the Elovich kinetic model ($R^2=0,898$). If the principal adsorption mechanism is chemical interaction, the $q_e = f(\ln t)$ plot is a straight line, whose slope and intercept determine rate coefficient α (mg/g min) and desorption constant β (mg/g) in Elovich kinetic model. Application of the pseudo-first kinetic model or intra-particle diffusion model gives lower correlation coefficients ($R^2=0,800$; and $R^2=0,669$ respectively (Table 2).

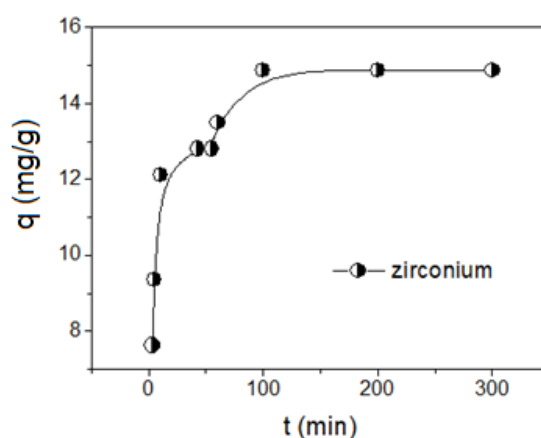


Figure.1. The effect of time interaction on zirconium ions adsorption by NaX (L: S=50, pH=7). The initial concentration of zirconium ions is 0,005M.

Table 2. Applying kinetic models to experimental results of zirconium adsorption by NaX.

Kinetic model	Adsorption equation	Relate coefficients	R ²
Diffusion	$q_t = 0,41t^{0,5} + 9,3$	$D_{ipd} = 0,41$	0,6689
Elovich	$q_t = 1,5\ln t + 7,1$	$\beta = 0,66$ $\alpha = 16,44$	0,898
Pseudo-first order	$\log (q_0 - q_t) = -0,0091t + 0,75$	$k_1 = 0,009$	0,8003
Pseudo-second order	$\frac{t}{q_t} = 0,066t + 0,32$	$k_2 = 0,066$	0,9992

The influence of zirconium equilibrium concentrations on its adsorption values by NaX is shown in Figure 2. Zirconium adsorption by zeolite NaX grows in the range of zirconium equilibrium concentrations 27 - 3000 mg/L. This process is well described by the Freundlich adsorption theory.

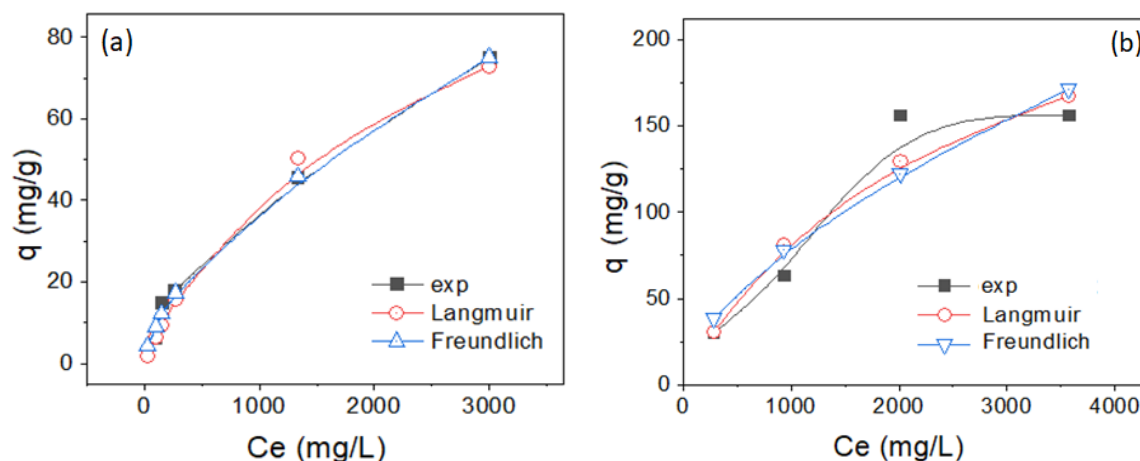


Figure.2. (a) Isotherm of adsorption of zirconium ions by NaX (L: S=50, pH=7), a nonlinear approximation of experimental adsorption isotherm by Langmuir and Freundlich adsorption theories; (b) Isotherm of strontium adsorption by NaX from aqueous solution in neutral medium.

Table 3. Nonlinear approximation of equilibrium adsorptions of Zr^{4+} and Sr^{2+} by NaX.

Cation	Theories	Parameters of equation	R^2	χ^2
Zr^{4+} $Q_{exp}=75$ mg/g	Langmuir	$A_{max}=113,96$ $K_L=0,000593$	0,9839	4,964
	Freundlich	$n=0,611$ $K_f=0,561$	0,9947	2,114
Sr^{2+} $Q_{exp}=156$ mg/g	Langmuir	$A_{max}=269,3$ $K_L=0,000461$	0,9077	10,19
	Freundlich	$n=0,588$ $K_f=1,39$	0,8669	15,38

Applying the Freundlich adsorption theory to the experimental results of zirconium adsorption by NaX gives higher R^2 values than the Langmuir adsorption theory. R^2 close to a unit (0,9947) indicates an adequate description of the zirconium adsorption onto NaX by the Freundlich adsorption theory (which is used to describe the experimental data of adsorption on heterogeneous surface, i.e., a surface with different types of adsorption centers [34]). This conclusion confirms a low chi-squared value ($\chi^2 = 2,114$) (Table 3). Experimental results of strontium adsorption, in contrast, are well described by Langmuir adsorption theory, which indicates that strontium is involved in adsorption centers of essentially the same type.

3.2. The effect of solution acidity and size of zeolite particles on zirconium ions adsorption.

The dependence of the adsorption value of the zirconium ions by NaX from solution acidity is shown in Figure 3. Adsorption values of zirconium by zeolite grows with the pH increase. The error of arithmetic mean decreases with increasing pH value. This fact shows that zirconium ions' dominant adsorption occurs in a neutral medium, in the chemical states of ZrO^{2+} or $HZrO_2^+$ [26].

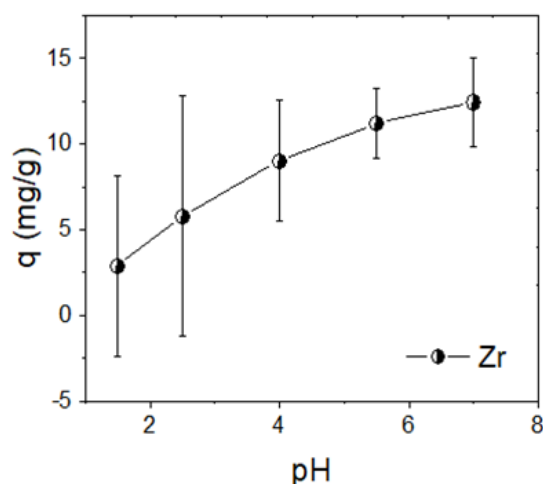


Figure 3. The dependence of the adsorption value of the zirconium ions by NaX from solution acidity (initial concentrations of zirconium ions were 0,001M. Error of arithmetic mean (percentage) of adsorption values calculated with a confidence level of 99%).

According to literature data, zirconium exists in the form of ZrO^{2+} in the range of pH values 2-7,5. Hydrated Zr(IV) exists as multiple monomeric and polynuclear oxy- and hydroxy-bridged species in solution at low pH due to its high charge and small radius [37]. Beyond pH =7,5 ZrO_2 precipitates in an insoluble form. Zirconium hydroxide does not interact with the surface of NaX because it has Lewis acid sites (accepted electrons) on the surface [38]. At the same time, NaX has acid sites of Brønsted acid sites (donated protons) and Lewis acid sites [30].

The dependence of adsorption values of zirconium ions on the size of zeolite particles is shown in Figure 4. Adsorption of zirconium ions is inversely proportional to the size of zeolite particles. Thus the maximum zirconium adsorption occurs where zeolite is in a powder form.

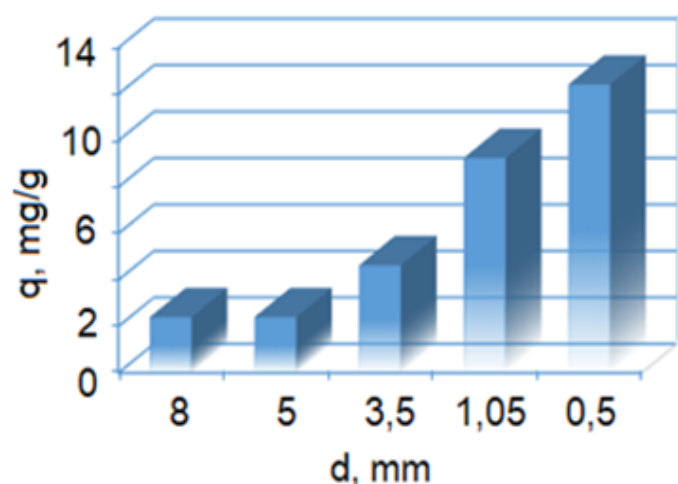


Figure 4. Dependence of zirconium adsorption values on particle size of NaX (mm), initial concentrations of zirconium ions is 0,001M, pH = 7.

3.3. Desorption of zirconium from zeolite surface. NaX dissolution in nitric acid.

The fluorescent X-ray analysis confirmed the presence of adsorbed zirconium (or strontium) on the NaX surface (Figures 5, 6, and 7, Table 4).

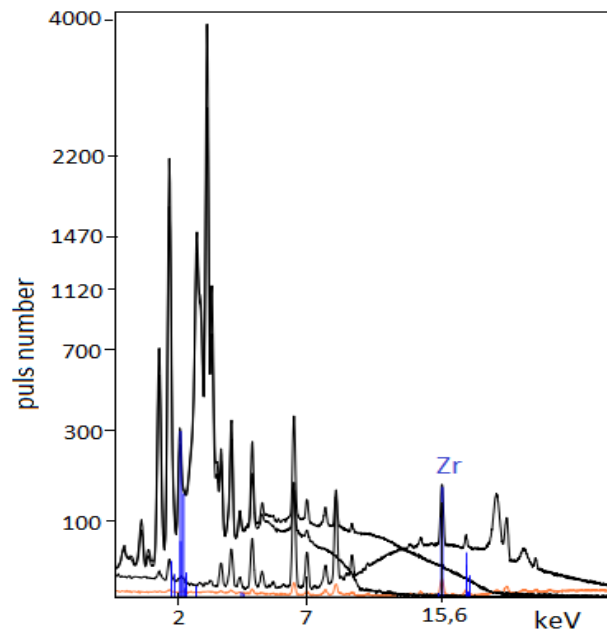


Figure 5. XRF spectrum of NaX with adsorbed zirconium on the surface.

Table 4. Relative content of oxides % (wt.) in NaX structure after adsorption of Zr⁴⁺ and Sr²⁺ ions.

% (wt.)	Na ₂ O	MgO	Al ₂ O ₃	SiO ₂	CaO	TiO ₂	Fe ₂ O ₃	Zr ⁴⁺	Sr ²⁺
1	55,7	13,5	11,2	10,7	1,05	0,374	0,319	0,28	0
2	53,7	8,31	6,18	12,3	2,71	0,298	0,708	<0,1	2,17

1. After zirconium adsorption; 2.-After strontium adsorption.

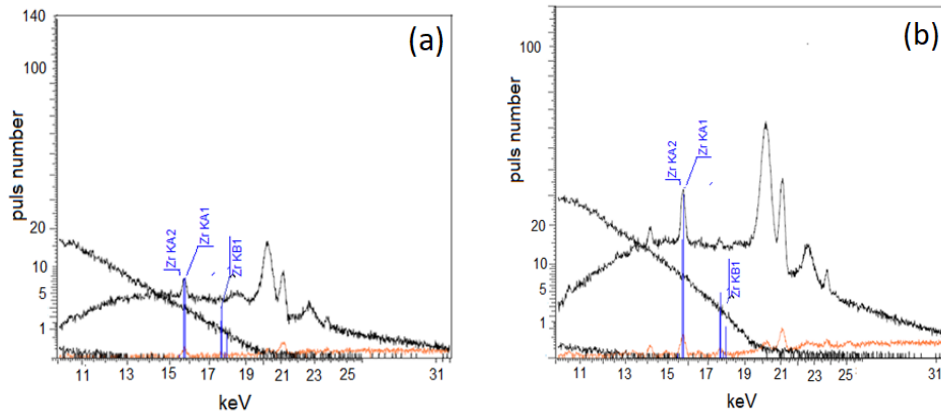


Figure 6. Part of XRF spectrum of NaX after desorption of zirconium ions: (a) by 10 % HNO₃; (b) by 10 ml 1% oxalic acid.

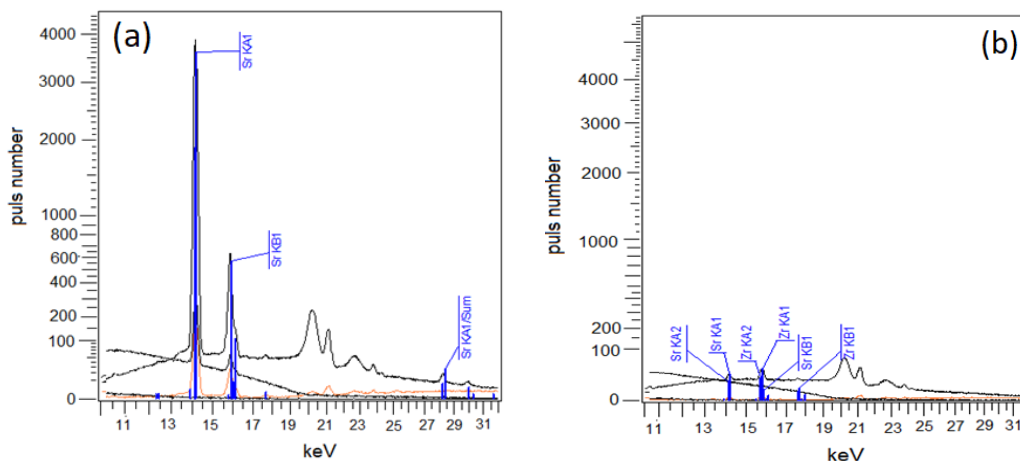


Figure 7. (a) Part of XRF spectrum of NaX samples with adsorbed strontium on the surface; (b) Part of XRF spectrum of NaX samples after 5 min of interaction with 10% HNO₃.

Figures 6 (a) and (b) show the nitric and oxalic acids' effectiveness in terms of zirconium desorption from the zeolite surface. 80 % of the total amount of adsorbed zirconium was eluted by 10 ml 1% H₂C₂O₄ and 94,67% - by 10 ml 10 % HNO₃. Meanwhile, nitric acid dilutes some elements of the zeolite structure together with zirconium.

Partial dissolution of NaX in nitric acid is described in Table 5.

Table 5. The changes of relative content % (wt.) of oxides in zeolite's structure under dissolution in nitric acid (t, min – duration of the interaction of NaX with concentrate HNO₃).

% (wt.) / T, min	Na ₂ O	MgO	Al ₂ O ₃	SiO ₂	CaO	TiO ₂	Fe ₂ O ₃
0	53,7	8,31	11,2	12,3	2,71	0,298	0,708
15	38,4	5,83	12,8	31,3	0,818	1,34	0,658
30	34,5	5,99	6,96	41,9	0,733	1,2	0,526
215	19,9	3,31	4,93	63,3	0,486	1,69	0,592
1440	23,5	0	2,66	63	0,66	2,27	0,724

The proportion of the SiO₂, TiO₂, and Fe₂O₃ oxides insoluble in nitric acid increases, the Al₂O₃ fraction decreases, and MgO is thoroughly washed out from the adsorbent matrix, as NaX zeolite degrades in concentrated HNO₃ (Table 5). Together with zirconium cations, Mg²⁺, Al³⁺, and Na⁺ cations are recovered from the zeolite structure. Point of zero charges of NaX surface (pH_{pzc}) is shifting from pH=11,5 to pH=2,3 after degradation NaX in acid medium, which lead to a decrease of zirconium adsorption. The decrease in zirconium adsorption may also be induced by the decrease in the number of sodium cations, some of which were exchangeable cations and were responsible for cation-exchange properties [38].

It is well known that the structure of faujasite is built of silicon layers (Si₂O₅) attached to similar aluminum hydroxide layers (Al(OH)₄), called Gibbsite layers by relatively weak bonds. Sometimes, zeolite works as a molecular sieve. Faujasite possesses super cages with a diameter near 10-13 Å. Their basic building block consists of a Si or Al atom in the tetrahedron center. This tetrahedron has oxygen in the four corners. Strontium, as a divalent cation, enters the inner sphere of zeolite [39-42] (Figure 8). This explains increased strontium adsorption by NaX. In contrast with strontium, the hydrated zirconium ions are very large in size [41, 42] and do not penetrate the inner NaX sphere. Under normal conditions, zirconium ions are adsorbed only by zeolite's surface in a neutral medium. When zirconium results from β⁻ decay of radioactive ⁹⁰Sr, or ⁹²Sr adsorbed by NaX (Figure 8), its interaction with NaX depends on the previous interaction of ⁹²Sr with the zeolite.

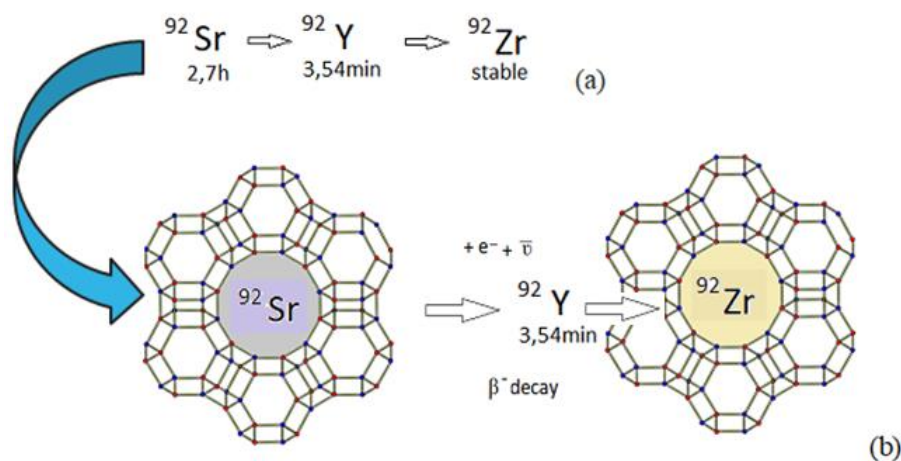


Figure 8. (a) Part of β⁻ decay chain of radionuclides with Ar=92; (b) strontium interaction with NaX. A schematic image of a zeolite supercage was built according to the literature [43].

If ^{92}Zr results from ^{92}Sr β -decay, it remains in the inner zeolite sphere. However, like strontium, it will be easily desorbed by concentrated HNO_3 since the acid destroys the zeolite itself.

4. Conclusions

The equilibrium in adsorption of zirconium ions by zeolite NaX establishes after 100 minutes of contact between zeolite surface and zirconium ions. Zirconium adsorption by zeolite NaX grows in the range of zirconium equilibrium concentrations of 27-3000 mg/L. The maximum experimental adsorption values of NaX toward zirconium and strontium cations are $75 \text{ mg}\cdot\text{g}^{-1}$ and $156 \text{ mg}\cdot\text{g}^{-1}$, respectively. The process of zirconium adsorption is well described by the Freundlich adsorption theory, while strontium adsorption is well described by Langmuir adsorption theory.

Zeolite NaX becomes chemically unstable at pH less than 4. The proportion of the SiO_2 , TiO_2 , and Fe_2O_3 oxides insoluble in nitric acid increases, the Al_2O_3 fraction decreases, and MgO is wholly removed from the adsorbent matrix, with the degradation of NaX in concentrated HNO_3 . The adsorbed radionuclides can be desorbed and re-released into the environment in an acid medium. If we suppose to use zeolite NaX as a carrier for radionuclides, special attention should be paid to this.

Funding

This work was supported by a research grant in Nuclear Forensics STCU [project 9906].

Acknowledgments

The authors are grateful to the librarians of Uzhgorod National University (Kyryliuk Nataly, Dankanych Oksana and Kobylitskiy V.) for their help in working on this publication. The authors are also grateful to Myslin Mariana to determine the point of zero charges of the zeolite surface.

Conflicts of Interest

The authors declare that they have no known competing financial interests or personal relationships that could have influenced the work reported in this paper.

References

1. Barrer, R.M.; Meier, W.M. Structural and ion sieve properties of a synthetic crystalline exchanger. *Trans. Faraday Society* **1958**, *54*, 1074-1085, <https://doi.org/10.1039/TF9585401074>.
2. Zhang, X.; Tang, D.; Zhang, M.; Yang, R. Synthesis of NaX zeolite: Influence of crystallization time, temperature and batch molar ratio $\text{SiO}_2/\text{Al}_2\text{O}_3$ on the particulate properties of zeolite crystals. *Powder Technol.* **2013**, *235*, 322-328, <https://doi.org/10.1016/j.powtec.2012.10.046>.
3. Fang, X.-H.; Fang, F.; Lu, C.-H.; Zheng, L. Removal of Cs^+ , Sr^{2+} , and Co^{2+} Ions from the Mixture of Organics and Suspended Solids Aqueous Solutions by Zeolites. *Nuclear Engineering and Technology* **2017**, *49*, 556-561, <https://doi.org/10.1016/j.net.2016.11.008>.
4. Ovhal, S.; Butler, I.; Xu, S. The Potential of Zeolites to Block the Uptake of Radioactive Strontium-90 in Organisms. *Contemporary Chemistry* **2018**, *1*.
5. Matsuda, M. Application 25 - Zeolite Membrane. In *Nanoparticle Technology Handbook (Third Edition)*, Naito, M., Yokoyama, T., Hosokawa, K., Nogi, K., Eds. Elsevier: 2018, 539-542, <https://doi.org/10.1016/B978-0-444-64110-6.00032-9>.

6. Jia, G.; Magro, L.; Torri, G.; Mariani, S. Sensitive and accurate methods for determination of low activity level of ^{90}Sr and ^{137}Cs in grass/vegetable samples. *Appl. Radiat. Isot.* **2021**, *169*, 109547, <https://doi.org/10.1016/j.apradiso.2020.109547>.
7. Vasylyeva, H.V., Mironyuk, I.F., Mykytyn, I.M. Adsorption of Co^{2+} and radioactive ^{60}Co by mesoporous TiO_2 . *Chemistry, physics and technology of surface.* **2019**, *10*, 446-457, <https://www.doi.org/10.15407/hftp10.04.446>.
8. Mironyuk, I., Tatarchuk, T., Vasylyeva, H., Naushad, M., Mykytyn, I. Adsorption of Sr(II) cations onto phosphated mesoporous titanium dioxide: Mechanism, isotherm and kinetics studies. *Journal of Environmental Chemical Engineering* **2019**, *7*, 103430, <https://www.doi.org/10.1016/j.jece.2019.103430>.
9. Mironyuk, I., Tatarchuk, T., Naushad, M., Vasylyeva, H., Mykytyn, I. Highly efficient adsorption of strontium ions by carbonated mesoporous TiO_2 . *J. Mol. Liq.* **2019**, *285*, 742-753, <https://www.doi.org/10.1016/j.molliq.2019.04.111>.
10. Kylyvnik Yu. M., Tryshyn V. V., Strilchuk M.V., Gaidar O.V., Vasylieva H.V., Vuchkan, S.I., Sych O.Ya., Syika, I.Yu. The titanium silicate influence on the Zn(II) and Sr(II) migration in the aquatic environment. *Nucl. Phys. At. Energy*, **2020**, *21*, 249-255, <https://doi.org/10.15407/jnpae2020.03.249>.
11. Abdel-Galil, E.A.; Hassan, R.S.; Eid, M.A. Assessment of nano-sized stannic silicomolybdate for the removal of ^{137}Cs , ^{90}Sr , and ^{141}Ce radionuclides from radioactive waste solutions. *Appl. Radiat. Isot.* **2019**, *148*, 91-101, <https://doi.org/10.1016/j.apradiso.2019.03.029>.
12. Mironyuk, I.F.; Gun'ko, V.M.; Vasylyeva, H.V.; Goncharuk, O.V.; Tatarchuk, T.R.; Mandzyuk, V.I.; Bezruka, N.A.; Dmytrotso, T.V. Effects of enhanced clusterization of water at a surface of partially silylated nanosilica on adsorption of cations and anions from aqueous media. *Microporous Mesoporous Mater.* **2019**, *277*, 95-104, <https://doi.org/10.1016/j.micromeso.2018.10.016>.
13. Mironyuk, I.F.; Mykytyn, I.M.; Kaglyan, O.Ye.; Gudkov, D.I.; Vasylyeva, H.V. ^{90}Sr adsorption from the aquatic environment of Chernobyl exclusion zone by chemically enhanced TiO_2 . *Nucl. Phys. At. Energy*, **2020**, *21*, 4, 347-353, <https://doi.org/10.15407/jnpae2020.04.347>.
14. Soltys, L.; Myronyuk, I.; Tatarchuk, T.; Tsinurchyn, V. Zeolite-based Composites as Slow Release Fertilizers (Review). *Physics and Chemistry of Solid State* **2020**, *21*, 89-104, <https://www.doi.org/10.15330/pcss.21.1.89-104>.
15. Takata, T.; Tsunoji, N.; Takamitsu, Y.; Sadakane, M.; Sano, T. Incorporation of various heterometal atoms in CHA zeolites by hydrothermal conversion of FAU zeolite and their performance for selective catalytic reduction of NO_x with ammonia. *Microporous Mesoporous Mater.* **2017**, *246*, 89-101, <https://doi.org/10.1016/j.micromeso.2017.03.018>.
16. Ezzeddine, Z.; Batonneau-Gener, I.; Pouilloux, Y.; Hamad, H.; Saad, Z. Synthetic NaX Zeolite as a Very Efficient Heavy Metals Sorbent in Batch and Dynamic Conditions. *Colloids and Interfaces* **2018**, *2*, <https://www.doi.org/10.3390/colloids2020022>.
17. Korkuna, O.; Lebeda, R.; Skubiszewska-Zieba, J.; Vrublevs'ka, T.; Gun'ko, V.M.; Ryczkowski, J. Structural and physicochemical properties of natural zeolites: clinoptilolite and mordenite. *Microporous Mesoporous Mater.* **2006**, *87*, 243-254, <https://doi.org/10.1016/j.micromeso.2005.08.002>.
18. Król, M. Natural vs. Synthetic Zeolites. *Crystals* **2020**, *10*, <https://doi.org/10.3390/cryst10070622>.
19. Levenets, V.V.; Lonin, A.Y.; Omelnik, O.P.; Shchur, A.O. Comparison the sorption properties of clinoptilolite and synthetic zeolite during sorption strontium from the water solutions in static conditions: Sorption and quantitative determination of strontium by the method PIXE. *Journal of Environmental Chemical Engineering* **2016**, *4*, 3961-3966, <https://www.doi.org/10.1016/j.jece.2016.09.011>.
20. Elboughdiri, N. The use of natural zeolite to remove heavy metals Cu (II), Pb (II) and Cd (II), from industrial wastewater. *Cogent Engineering* **2020**, *7*, 1782623, <https://doi.org/10.1080/23311916.2020.1782623>.
21. Esmaeili, A.; Mobini, M.; Eslami, H. Removal of heavy metals from acid mine drainage by native natural clay minerals, batch and continuous studies. *Applied Water Science* **2019**, *9*, 97, <https://doi.org/10.1007/s13201-019-0977-x>.
22. Taamneh, Y.; Sharadqah, S. The removal of heavy metals from aqueous solution using natural Jordanian zeolite. *Applied Water Science* **2017**, *7*, 2021-2028, <https://doi.org/10.1007/s13201-016-0382-7>.
23. Zolfonoun, E.; Monji, A.B.; Taghizadeh, M.; Ahmadi, S.J. Selective and direct sorption of zirconium from acidic leach liquor of zircon concentrate by rice bran. *Miner. Eng.* **2010**, *23*, 755-756, <https://doi.org/10.1016/j.mineng.2010.05.005>.
24. O'Hara, M.J.; Murray, N.J.; Carter, J.C.; Kellogg, C.M.; Link, J.M. Tandem column isolation of zirconium-89 from cyclotron bombarded yttrium targets using an automated fluidic platform: Anion exchange to

- hydroxamate resin columns. *J. Chromatogr.* **2018**, *1567*, 37-46, <https://doi.org/10.1016/j.chroma.2018.06.035>.
25. O'Hara, M.J.; Murray, N.J.; Carter, J.C.; Kellogg, C.M.; Link, J.M. Hydroxamate column-based purification of zirconium-89 (⁸⁹Zr) using an automated fluidic platform. *Appl. Radiat. Isot.* **2018**, *132*, 85-94, <https://doi.org/10.1016/j.apradiso.2017.10.048>.
 26. Bhatt, N.B.; Pandya, D.N.; Wadas, T.J. Recent Advances in Zirconium-89 Chelator Development. *Molecules* **2018**, *23*, <http://dx.doi.org/10.3390/molecules23030638>.
 27. Akolekar, D.; Chaffee, A.; Howe, R.F. The transformation of kaolin to low-silica X zeolite. *Zeolites* **1997**, *19*, 359-365, [https://www.doi.org/10.1016/S0144-2449\(97\)00132-2](https://www.doi.org/10.1016/S0144-2449(97)00132-2).
 28. Bondareva, G.V.; Rat'ko, A.I.; Azarov, S.M. Hydrothermal Synthesis of Zeolite NaX on Porous Ceramic Supports. *Inorg. Mater.* **2003**, *39*, 605-609, <https://www.doi.org/10.1023/A:1024053304236>.
 29. Hamilton, K.E.; Coker, E.N.; Sacco, A.; Dixon, A.G.; Thompson, R.W. The effects of the silica source on the crystallization of zeolite NaX. *Zeolites* **1993**, *13*, 645-653, [https://doi.org/10.1016/0144-2449\(93\)90137-R](https://doi.org/10.1016/0144-2449(93)90137-R).
 30. Sadeghbeigi, R. Chapter 4 - FCC Catalysts. In *Fluid Catalytic Cracking Handbook (Third Edition)*, Sadeghbeigi, R., Ed. Butterworth-Heinemann: Oxford, 2012; <https://doi.org/10.1016/C.2010-0-67291-9>.
 31. Hartman, R.L.; Fogler, H.S. Understanding the Dissolution of Zeolites. *Langmuir* **2007**, *23*, 5477-5484, <https://www.doi.org/10.1021/la063699g>.
 32. Mironyuk, I.; Tatarchuk, T.; Vasylyeva, H.; Gun'ko, V.M.; Mykytyn, I. Effects of chemisorbed arsenate groups on the mesoporous titania morphology and enhanced adsorption properties towards Sr(II) cations. *J. Mol. Liq.* **2019**, *282*, 587-597, <https://doi.org/10.1016/J.MOLLIQ.2019.03.026>.
 33. Vasylyeva, H.; Mironyuk, I.; Mykytyn, I.; Savka, K. Equilibrium studies of yttrium adsorption from aqueous solutions by titanium dioxide. *Appl. Radiat. Isot.* **2021**, *168*, 109473, <https://doi.org/10.1016/j.apradiso.2020.109473>.
 34. Tran, H.N.; You, S.-J.; Hosseini-Bandegharai, A.; Chao, H.-P. Mistakes and inconsistencies regarding adsorption of contaminants from aqueous solutions: A critical review. *Water Res.* **2017**, *120*, 88-116, <https://doi.org/10.1016/j.watres.2017.04.014>.
 35. Tran, H.N.; Tomul, F.; Thi Hoang Ha, N.; Nguyen, D.T.; Lima, E.C.; Le, G.T.; Chang, C.-T.; Masindi, V.; Woo, S.H. Innovative spherical biochar for pharmaceutical removal from water: Insight into adsorption mechanism. *J. Hazard. Mater.* **2020**, *394*, 122255, <https://www.doi.org/10.1016/j.jhazmat.2020.122255>.
 36. Standard Deviation Calculator. Available online: <http://www.calculator.net/standard-deviation-calculator.html>
 37. Deri, M.-A. Zirconium-89: Radiochemistry and Ligand Development toward Improved PET Applications. A dissertation submitted to the Graduate Faculty in Chemistry in partial fulfillment of the requirements for the degree of Doctor of Philosophy, Graduate Center, City University of New York, **2015**.
 38. Mironyuk, I.; Mykytyn, I.; Vasylyeva, H.; Savka, K. Sodium-modified mesoporous TiO₂: Sol-gel synthesis, characterization and adsorption activity toward heavy metal cations. *J. Mol. Liq.* **2020**, *316*, 113840, <https://www.doi.org/10.1016/j.molliq.2020.113840>.
 39. Munthali, M.W.; Johan, E.; Aono, H.; Matsue, N. Cs⁺ and Sr²⁺ adsorption selectivity of zeolites in relation to radioactive decontamination. *Journal of Asian Ceramic Societies* **2015**, *3*, 245-250, <https://www.doi.org/10.1016/j.jascer.2015.04.002>.
 40. Mimura, H.; Kanno, T. Distribution and Fixation of Cesium and Strontium in Zeolite A and Chabazite. *J. Nucl. Sci. Technol.* **1985**, *22*, 284-291, <https://www.doi.org/10.1080/18811248.1985.9735658>.
 41. Martínez, C.; Corma, A. 5.05 - Zeolites. In *Comprehensive Inorganic Chemistry II (Second Edition)*, Reedijk, J., Poeppelemeier, K., Eds. Elsevier: Amsterdam, 2013; 103-131, <https://doi.org/10.1016/B978-0-08-097774-4.00506-4>.
 42. Busca, G. Chapter 7 - Zeolites and Other Structurally Microporous Solids as Acid-Base Materials. In *Heterogeneous Catalytic Materials*, Busca, G., Ed. Elsevier: Amsterdam, 2014; 197-249, <https://doi.org/10.1016/B978-0-444-59524-9.00007-9>.
 43. Feng, R.; Yan, X.; Hu, X.; Qiao, K.; Yan, Z.; Rood, M.J. High performance of H₃BO₃ modified USY and equilibrium catalyst with tailored acid sites in catalytic cracking. *Microporous Mesoporous Mater.* **2017**, *243*, 319-330, <https://doi.org/10.1016/j.micromeso.2017.02.041>.